Articles

Modulating Retinoid X Receptor with a Series of (*E*)-3-[4-Hydroxy-3-(3-alkoxy-5,5,8,8-tetramethyl-5,6,7,8-tetrahydronaphthalen-2-yl)phenyl]acrylic Acids and Their 4-Alkoxy Isomers†

Efrén Pérez Santín,[||] Pierre Germain,[§,⊥] Fabien Quillard,[‡] Harshal Khanwalkar,[⊥] Fátima Rodríguez-Barrios,[||] Hinrich Gronemeyer,*[,⊥] Ángel R. de Lera,*[,||] and William Bourguet*[,‡,§]

INSERM, U554, 34090 Montpellier, France, Université Montpellier 1 et 2, CNRS, UMR5048, Centre de Biochimie Structurale, 34090 Montpellier, France, Departamento de Química Orgánica, Facultad de Química, Universidade de Vigo, 36310 Vigo, Spain, Institut de Génétique et de Biologie Moléculaire et Cellulaire (IGBMC), BP 10142, 67404 Illkirch Cedex, C. U. de Strasbourg, France

Received January 23, 2009

Rexinoids are ligands for the retinoid X receptor (RXR) that have great promise for both the prevention and treatment of cancer and metabolic diseases. In this regard, synthetic, functional, and structural investigations into the structure−activity relationships of derivatives of the potent RXR agonist (*E*)-3-[3-(3,5,5,8,8-pentamethyl-5,6,7,8-tetrahydronaphthalen-2-yl)-4-hydroxyphenyl]acrylic acid (CD3254, **9**) have been conducted. We recently reported on the characterization of a series of C3′-substituted alkyl ether analogues of **9** (**10a**−**f**), which display activities ranging from partial agonists to pure antagonists. The importance of the position of the alkoxy side chain for ligand activity has been further explored with the synthesis of C4′-substituted analogues (**11a**−**f**). Here we describe the synthesis of compounds **11a**−**f**, which appear functionally different from their isomeric counterparts, as judged from transactivation assays and fluorescence anisotropy experiments. We also report on the 2.0 Å resolution structure of RXR in complex with the parent compound **9**, which helps understanding of the impact of the alkyl side chain location on ligand activity.

Introduction

Retinoid X receptors (RXRs), comprising isotypes α, *β*, and *γ*, are members of the nuclear receptor (NR[a]) superfamily of transcriptional regulators.[1,2] Although they are activated by 9-*cis*-retinoic acid and other ligands such as docosahexaenoic acid (DHA),[3] the true physiological ligand, if existing, remains to be identified.[4] Ligand binding regulates cognate gene transcription by a still incompletely understood sequence of events that are initiated upon NR binding to *cis*-acting DNA response elements, involve chromatin modification and remodeling, and ultimately lead to recruitment of the transcription machinery. RXR plays a central role in nuclear receptor signaling because it is the common heterodimerization partner of multiple nuclear receptors.[5] The mechanism of gene regulation through heterodimers is highly complex, and functional details are emerging only slowly.[6] Recent studies revealed that gene regulation by pure RXR ligands (termed rexinoids) depends on the nature and the status (ligand-bound or unbound) of the RXR heterodimerization partner. Thus, in the context of retinoic acid receptor (RAR)−RXR heterodimers, RAR agonists can autonomously activate transcription but RXR responds to rexinoids only in the presence of a RAR ligand.[7] Recently, RXRs have been shown to bind ligands and recruit coactivators in unliganded (apo)-RAR heterodimers but are unable to activate transcription because the corepressor does not dissociate (RXR "subordination").[8] The mechanism of RXR subordination in RAR−RXR heterodimers does not apply to a group of nuclear receptors (FXR, LXR, PPAR,...), which form so-called "permissive" heterodimers.[9,10] For example, both RXR as well as peroxisome proliferator activated receptor (PPAR) agonists activate PPAR−RXR heterodimers, which enables rexinoids to function as insulin sensitizers in rodent models of noninsulin-dependent diabetes mellitus.[11] This illustrates the potential therapeutic implications of RXR-selective ligands in combination with other modulators of the nuclear receptor superfamily to activate−inactivate the heterodimers and regulate diverse hormonal pathways.[12,13]

In contrast to the fairly large collection of RXR agonists known to date,[14,15] only a few RXR antagonists have been reported.[16] (2*E*,4*E*,6*Z*)-7-[5,5,8,8-tetramethyl-5,6,7,8-tetrahydro-2-(*n*-propoxy)naphthalen-3-yl]-3-methylocta-2,4,6-trienoic acid (LG100754) acts as an RXR homodimer antagonist but is also an agonist of several RXR heterodimers (Figure 1).[17] (2*E*,4*E*,6*Z*)-7-[3,5-Di-*tert*-butyl-2-(2,2-difluoroethoxy)phenyl]-3-methylocta-2,4,6-trienoic acid (LG101506) shows a homodimer antagonistic profile as well and synergizes with PPAR*γ* agonists to enhance

† PDB ID Code: The atomic coordinates of the RXRα/CD3254 complex have been deposited in the Protein Data Bank under the accession code 3FUG.

* To whom correspondence should be addressed. For W.B.: phone, +(33) 4 67 41 7702; fax, +(33) 4 67 41 7913; E-mail: bourguet@cbs.cnrs.fr. For H.G.: phone, +(33) 3 88 65 3473; fax, +(33) 3 88 65 3437; E-mail, hg@igbmc.u-strasbg.fr. A.R.de L.: phone, +(34) 9 86 81 2316; fax, +(34) 9 86 81 1940; E-mail, qolera@uvigo.es.

‡ INSERM.

§ Université Montpellier 1 et 2, CNRS, UMR5048, Centre de Biochimie Structurale.

|| Departamento de Química Orgánica, Facultad de Química, Universidade de Vigo.

⊥ Institut de Génétique et de Biologie Moléculaire et Cellulaire (IGBMC).

[a] Abbreviations: NR, nuclear receptor; RXR, retinoid X receptor; RAR, retinoic acid receptor; SRC-1, steroid receptor coactivator 1; TIF-2, transcriptional intermediary factor 2.

10.1021/jm900096q CCC: $40.75
Published on Web 05/01/2009

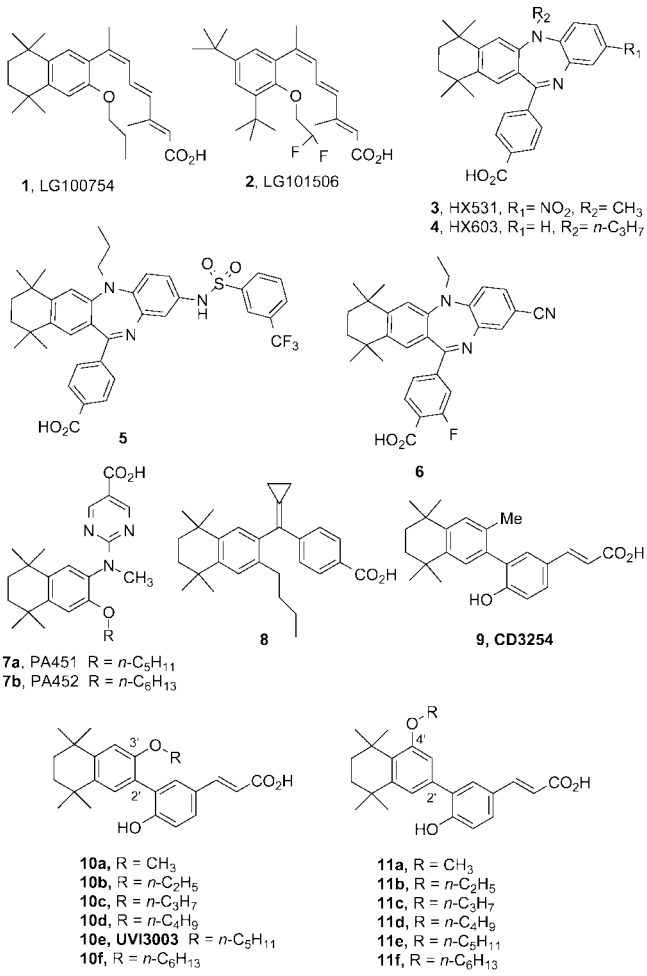

Figure 1. RXR antagonists. The series of RXR modulators discussed in the present report (**10a**−**f** and **11a**−**f**), which are derived from the parent agonist **9**, are also depicted.

activation at the PPARγ−RXR heterodimer but does not synergize with the RAR ligand (*E*)-4-(2-(5,5,8,8-tetramethyl-5,6,7,8-tetrahydronaphthalen-2-yl)prop-1-enyl)benzoic acid (TTNPB) to enhance activation at the RAR−RXR heterodimer.[18,19] The polyene structures of LG100754 (**1**) and LG101506 (**2**) is replaced by more rigid skeletons in 4-(5,7,7,10,10-pentamethyl-2-nitro-7,8,9,10-tetrahydro-5*H*-benzo[*b*]naphtho[2,3-*e*][1,4]diazepin-12-yl)benzoic acid (HX531) and 4-(7,7,10,10-tetramethyl-5-propyl-7,8,9,10-tetrahydro-5*H*-benzo[*b*]naphtho[2,3-*e*][1,4]diazepin-12-yl)benzoic acid (HX603), which are inhibitors of RXR heterodimers, but also inhibit the activation of RARs by agonists.[20] Two other diazepinyl benzoic acids related to HX531 (**3**) and HX603 (**4**) are sulfonamide (**5**)[21] and cyano derivative (**6**), which showed improved oral bioavailability and potency.[22] 2-[(3-Pentyloxy-5,5,8,8-tetramethyl-5,6,7,8-tetrahydronaphthalen-2-yl)(methylamino)]pyrimidine-5-carboxylic acid (PA451) and 2-[(3-hexyloxy-5,5,8,8-tetramethyl-5,6,7,8-tetrahydronaphthalen-2-yl)(methylamino)]pyrimidine-5-carboxylic acid (PA452) are specific inhibitors of retinoid synergism in RAR−RXR heterodimers.[23] A rationale for the antagonism of compounds **3**, **4**, PA451 (**7a**), and PA452 (**7b**) based on the inhibition of folding of H12 has been put forward.[16] In contrast, cyclopropylidene derivative (**8**) was shown to block RARβ expression induced by the PPARγ−RXRα heterodimer via inhibition of 9-*cis*-retinoic acid induced recruitment of coactivator SRC-1 to RXRα.[24]

RXR-selective antagonists are useful tools for the elucidation of the complex gene networks governed by the nuclear hormone heterodimers, and their potential clinical application has been highlighted.[25,12] We recently reported[26] a new series of RXR modulators **10a**−**f** based on the structure of CD3254 (**9**),[27] a potent and selective RXR agonist (Figure 1). Docking studies suggested that replacing the methyl substituent at the C3′ position of **9** by an extended alkyl ether side chain might prevent helix H12 of the receptor from adopting its agonist conformation, in line with current mechanistic views of the antagonistic action of nuclear receptor ligands.[16,28,29] Indeed, a series of alkoxy analogues of **9** with chains from one to six carbon atoms (**10a**−**f**) exhibited properties ranging from agonist to partial agonist to antagonist (in particular, (*E*)-3-[3-(5,5,8,8-tetramethyl-5,6,7,8-tetrahydro-3-(pentyloxy)naphthalen-2-yl]-4-hydroxyphenyl]acrylic acid, UVI3003) depending on the length of the alkyl chain. It was thus reasonable to assume that the biological activities of **10a**−**f** resulted from a modulation of H12 positioning induced by the size of the substituent. Indeed, crystallographic and fluorescence anisotropy analyses fully supported this concept. Either mediated through a water molecule (**10a**,**b**) or by a steric clash with the longer alkyl chains (**10b**−**d**), the reorientation of the H11 residue L436 was proposed to affect the dynamics of helix H12 and thereby to account for the mixed agonist/antagonist activity of the corresponding ligands. In contrast, a direct interaction between the side chains of UVI3003 (**10e**) and **10f** and H12 was considered to give rise to the antagonistic profile of these compounds.[26]

Here we report on the chemical synthesis and receptor activation profiles of a isomeric series of tetramethyltetrahydronaphthalene cinnamic acids **11a**−**f** in which the alkoxy chain is attached to the C4′ position (Figure 1). A new synthesis of the parent compound **9** is also described. Moreover, we disclose the crystal structure of RXRα LBD bound to **9** that helps explain the divergent activities of the C3′ and C4′-substituted series of ligands.

Results and Discussion

Chemistry. Synthesis of the biaryl[30] bond of agonist **9** was based on the Suzuki−Miyaura cross-coupling, known to be tolerant of steric hindrance in the aryl components.[31] Treatment of known[32] boronic acid **12** and 3-bromo-4-hydroxybenzaldehyde **13** yielded aldehyde **14** in low yield (25%). The alternative route involving phenol protection (Ac_2O, Py, DMAP) followed by olefin formation (NaH, triethylphosphonoacetate, DME, −30 °C) of acetate **15** was more efficient and provided compound **16** in high yield (95%). Heating boronic acid **12** and bromide **16** to 150 °C in the presence of $Pd(OAc)_2$, aqueous Na_2CO_3, and the phase transfer agent TBAB[33] resulted in a mixture of phenol **17** and acetate **18** in 97% yield (based on recovered **16**). These compounds were separated and characterized at this stage, but for synthetic convenience, the mixture was carried on to provide **9** by saponification (Scheme 1).

The synthesis of ethers **11a**−**f** started with the etherification of known[27] bromotetrahydronaphthol **19** under classical conditions (NaH, alkyliodide, DMF, 25 °C). Bromine−lithium exchange of **20** (*n*-BuLi, −78 °C),[34] followed by trapping each organolithium with triisopropylborate, furnished boronic acids **21**.[27] These were characterized and stored as the crystalline diethanolamine boronates **22**,[35] and the boronic acids were released from derivatives **22** by treatment with HCl in THF prior to use. The coupling of **21** to cinnamic ester **16** required refluxing in DME with catalytic quantities of $Pd(PPh_3)_4$ and excess Na_2CO_3 and provided the entire skeleton of the rexinoids as free phenols **23**. Saponification of the acrylic esters gave the

Scheme 1[a]

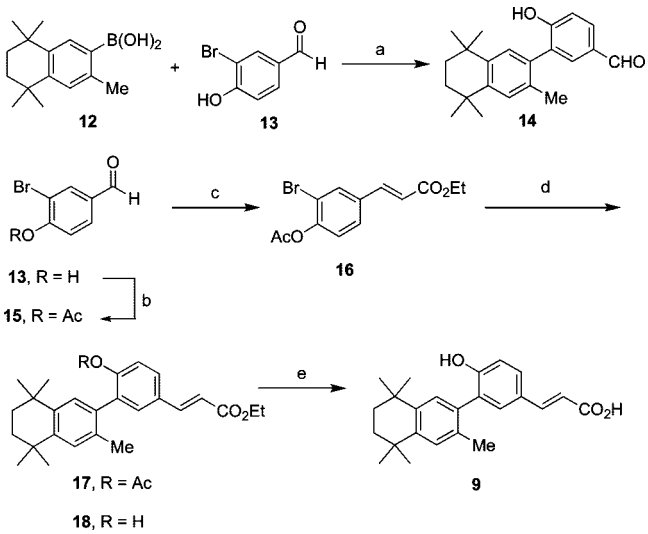

[a] Reagents and reaction conditions: (a) $Pd(PPh_3)_4$, aq Na_2CO_3, 60 °C, 25%; (b) Ac_2O, Py, DMAP, 4 h, 25 °C, 99%; (c) NaH, $(EtO)_2POCH_2CO_2Et$, DME, −30 °C, 1.5 h, 95%; (d) boronic acid **12**, $Pd(OAc)_2$, aq Na_2CO_3, TBAB, 150 °C, 97% (brsm); (e) LiOH, dioxane/H_2O, 60 °C, 85%.

desired compounds **11a**−**f** in high yields (Scheme 2). The synthesis of series **10a**−**f** has been described following a similar sequence.[26]

Fluorescence Anisotropy Studies. Using fluorescence anisotropy measurements of a fluorescein moiety that had been attached selectively to the C-terminus of RXR helix H12, we previously reported experimental evidence for a correlation between the pharmacological activity of modulators **10a**−**f** (Figure 1) and their impact on the structural dynamics of the activation helix H12.[26] Using the same approach, we observed that the novel series of compounds **11a**−**f** increases the mobility of helix H12, as revealed by the decreased anisotropy in the presence of these compounds relative to that seen for the full-agonist **9** (Figure 2A).

These data indicate that compounds **11a**−**f** fail to efficiently stabilize the active receptor conformation and suggest that they may act as partial agonists or antagonists. However, compound **10e** (Figure 1), which was previously characterized as a full-RXR antagonist,[26] destabilized holo-H12 significantly more than **11e**, suggesting that the latter is a less potent antagonist (or a more potent partial agonist) than the corresponding isomeric ligand **10e** (Figure 2A). To unambiguously differentiate partial agonists from full antagonists, we previously demonstrated that monitoring H12 dynamics in the presence of both ligands and a coactivator fragment is required.[26] We added increasing concentrations of a 13-residue peptide corresponding to the nuclear receptor box 2 region of the transcriptional intermediary factor 2 (TIF-2 NR2) and measured the resulting anisotropy for the various RXR/ligand complexes. In the presence of the agonist **9**, the addition of TIF-2 NR2 rapidly increased anisotropy and helix H12 appears fully stabilized at a peptide concentration of 1 μM (Figure 2B). By contrast, with ligands **11a**−**f**, anisotropy values increased gradually upon TIF-2 NR2 addition and helix H12 remained more dynamic, even at the highest peptide concentration used. Comparison of these data with those obtained with the isomeric series **10a**−**f** (Figure 1) revealed that the trends in compound behavior across the two homologous series were clearly different. Figure 2C shows that ligands **10a**−**f** generate large variations of anisotropy in response to the addition of TIF-2 NR2. The partial agonists **10a**−**d** induce graded receptor dynamics as indicated by the peptide concentration required for full stabilization of H12, which correlates inversely with the length of the aliphatic side chain. The antagonists **10e** and **10f** display a very different profile as even the highest doses of peptide fail to stabilize H12 completely. Conversely, ligands **11a**−**f** induced a more restricted range of receptor dynamics and higher peptide concentrations are required to reach the stabilization level obtained with the corresponding compounds in the **10a**−**f** series. Finally, neither **11e** nor **11f** displayed the dynamic profile observed for the full-antagonists **10e-f**. Together, these fluorescence anisotropy data reveal that compounds **11a**−**f** exhibit the dynamics signature of weak partial agonists whose degree of agonism slightly varies according to the side-chain length.

Functional Studies. Fluorescence anisotropy studies revealed that all compounds of the new series do bind to RXR and impinge on H12 dynamics. To assess the impact of this binding on RXR-mediated transcription activation in intact cells, we used

Scheme 2[a]

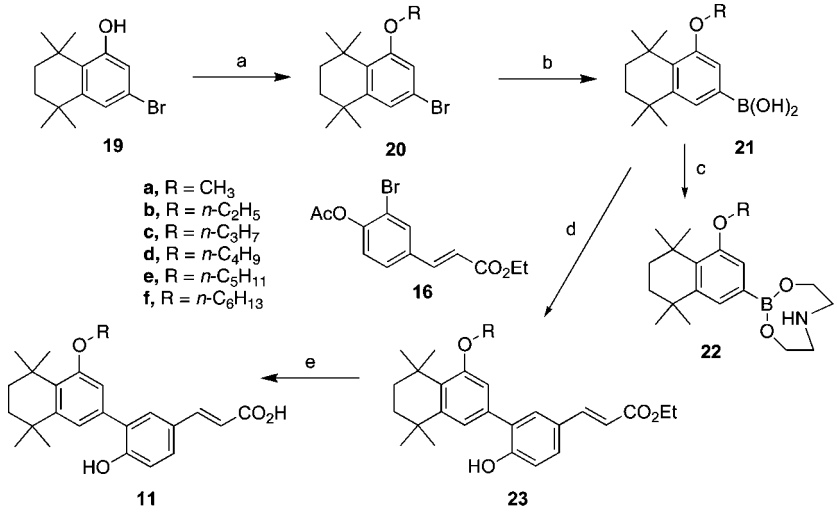

[a] Reagents and reaction conditions: (a) NaH, RI, DMF, 25 °C (**20a**, 92%; **20b**, 92%; **20c**, 93%; **20d**, 97%; **20e**, 96%; **20f**, 98%); (b) *n*-BuLi, TMEDA, $B(O^iPr)_3$, THF, 1 h (**21a**, 69%; **21b**, 84%; **21c**, 79%; **21d**, 78%; **21e**, 71%; **21f**, 81%); (c) diethanolamine, THF, 25 °C, 1 h, quant; (d) $Pd(PPh_3)_4$, 3M Na_2CO_3, DME, reflux (**23a**, 57%; **23b**, 71%; **23c**, 72%; **23d**, 68%; **23e**, 63%; **23f**, 64%); (e) 2 M KOH, MeOH, reflux (**11a**, 99%; **11b**,88%; **11c**, 100%; **11d**, 100%; **11e**, 93%; **11f**, 79%).

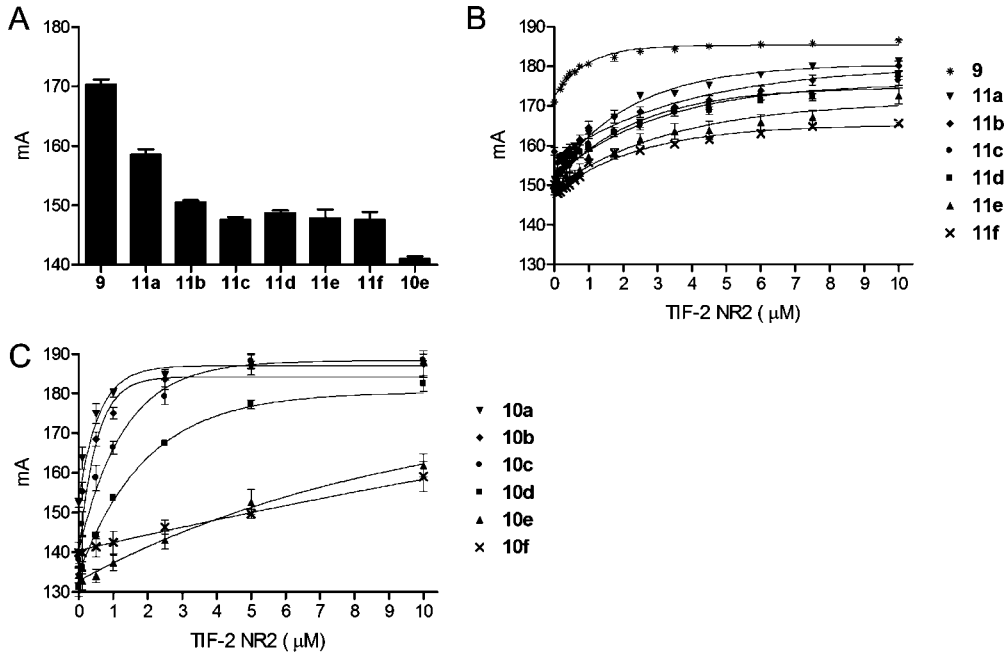

Figure 2. Ligand-induced RXRα helix H12 dynamics monitored by fluorescence anisotropy. (A) Using an RARα−RXRα LBD heterodimer in which a fluorescent dye is specifically attached to the C-terminus of RXRα, we measured anisotropy values in the presence of saturating concentrations of the series of mixed agonists/antagonists **11a**−**f**. For comparison, we also measured the effect of both the full-RXR agonist **9** and the previously reported full-antagonist **10e**. (B) Similar experiments were carried out in the presence of increasing concentrations of the NR interaction motif 2 peptide of the coactivator TIF-2 (LxxLL). (C) Same experiment as in (B) but using the previously described isomeric series of compounds **10a**−**f**.

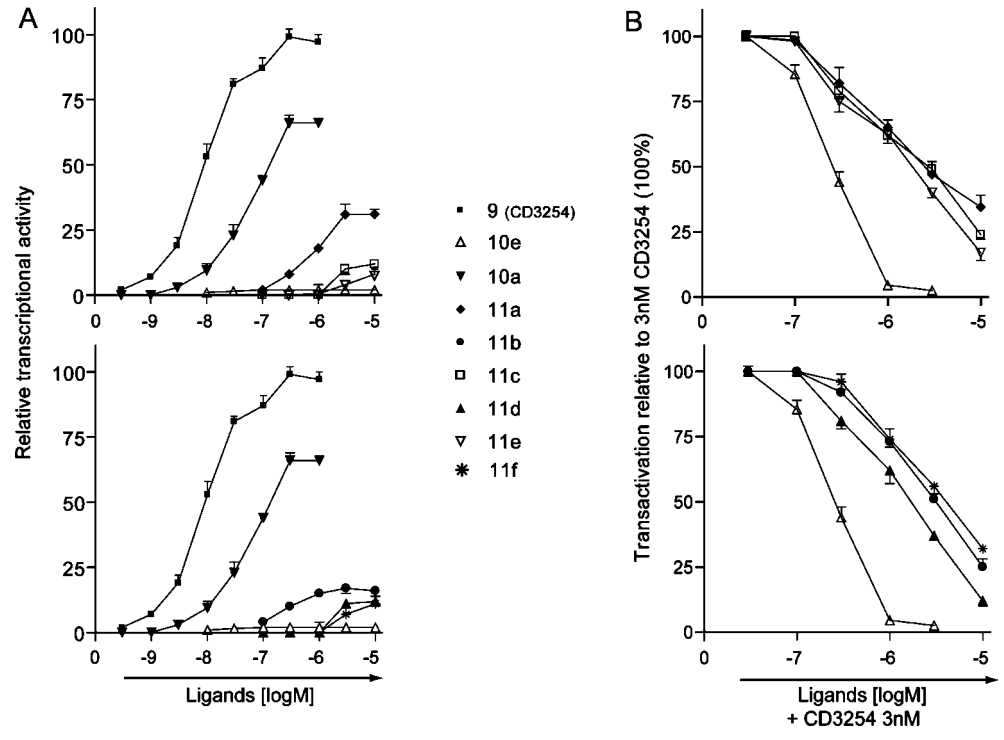

Figure 3. RXR agonist/antagonist potential of new compounds. HeLa cells stably transfected with the reporter recombinant 5xGal4-βGlo-Luc and Gal4-hRXRβ were incubated with increasing concentrations of compounds to assess their RXR agonist potential (A) or with 3 nM of **9** and increasing concentrations of the compounds to assess their RXR antagonist potential (B).

reporter assays with genetically engineered HeLa cell lines. These "reporter cells" express a chimeric receptor comprising the ligand binding domain of RXRβ fused to the DNA binding domain of the yeast GAL4 transcription factor. In addition, they contain a stably integrated chimeric promoter luciferase reporter, composed of five GAL4 response elements in front of a minimal β-globin promoter.

By establishing dose−response curves with this cellular model the relative potencies of the newly synthesized compounds for activating transcription of a cognate target gene were compared to that of **9** and **10e**; note that the latter have been characterized previously as pure RXR agonist and antagonist, respectively, with a high RXR binding affinity.[26] In all cases, the new compounds acted as weak agonists compared to **9** (Figure 3A).

Hence addition of the alkyl ether in the C4′ position provokes a major loss of transactivation efficacy of the corresponding holo-RXR. **11a**, which harbors the smallest substitution (Figure 1), is the most active of the series, displaying about 30% of the **9**-induced transactivation. Further extension of the side chain reduced the transactivation capacity of the rexinoid such that **11c**−**f** induced only about 10% of the reporter activity seen with **9**. However these C4′-substituted compounds acted always as partial agonists as they induced significant RXR activity, while the corresponding C3′-substituted **10e** was always inactive.

Competition curves derived from challenging 3 nM **9** with increasing ligand concentrations confirmed these results (Figure 3B). While **10e** is a potent full antagonist for **9**-induced transcription through Gal4-RXR, the new compounds provided very similar competition curves and showed that all these molecules antagonize **9**-induced transcription for RXR. Taken together the observations that (i) the activation curves of compounds **11a**−**f** are shifted toward higher concentrations (Figure 3A), (ii) **9**-induced RXR activation is quantitatively inactivated (Figure 3B) only at compound concentrations at or above 10 μM, and (iii) **10e** induced this level of antagonism already at a 10-fold lower concentration, it is highly likely that **11a**−**f** possess significantly lower affinity to RXR.

With respect to its abilities to act as partial agonists, i.e., to exhibit both weak agonist and antagonist potential (relative to the natural or a pure agonist), this series of C4′ substituted derivatives yielded partial RXR agonists that are poorly distinguishable from each other. Hence the alkoxy chains decrease in RXR transcriptional potential and generate ligands with a modest RXR affinity. While the previous analysis of C3′ alkyl ether-substituted rexinoids revealed a progressive transition from agonist via mixed agonist/antagonist to full antagonist which depended on the length of the aliphatic chain, no such effect is observed for the present C4′ substitutions. Apparently, the length of the alkyl ether attached to the C4′ position is not critical and poorly discriminatory.

Structural Studies. To provide structural evidence that can help to understand the different functionalities of the two isomeric series of RXR modulators, the RXRα LBD was crystallized with the parent compound **9** and the 13-residue peptide comprising the nuclear receptor-binding surface NR2 of the p160 coactivator family TIF-2 (also termed GRIP1 and SRC2). The structure refined at 2.0 Å resolution (Table 1) reveals the canonical ternary fold of NR LBDs in the active conformation (Figure 4A) and an unambiguous experimental $2F_o - F_c$ electron density map for the agonist **9** (Figure 4B). Figures 4A and 5A show that **9** occupies a similar location in the ligand-binding pocket (LBP) and adopts a similar binding mode as other RXR agonists.[36−38] The methyl group (C3′ position), which was replaced by a linear alkoxy substituent in the **10a**−**f** series (Figure 1), points toward a small cavity formed by residues C269, A272, L436, I447, and L451 (Figure 5A).

As exemplified by the structure of the RXR LBD/**10c** complex,[26] this cavity can accommodate medium-size aliphatic side-chains (1−4 carbon atoms), provided that L436 (H11) undergoes a significant conformational change (Figure 5B). However, the repositioning of L436 has been shown to account for the weak agonist activity of compounds **10a**−**d** by generating a steric clash with L455 from holo-H12.[26] In the same line, the structure of RXR LBD bound by **9** reaffirms the pivotal role of L436 in stabilizing holo-H12, as the conformation of this residue is identical to that observed in all structures of RXR complexed with a full agonist. In the **11a**−**f** series, the alkoxy chain is attached to the C4′ position as compared to the C3′ position in the **10a**−**f** isomers (Figure 1). Modeling studies reveal that the C4′ substitution points toward a space in the LBP that is partially occupied by residues V265, C269, L436, and F439 (Figure 5C). To accommodate the aliphatic extension, several residue side chains (F313, F346, H435, L436, F439) must therefore undergo significant conformational changes. It is thus predicted that, similarly to what was observed for the **10a**−**f** series, the displacement of the L436 side chain toward L455 (H12) accounts for the weak agonist activity of the novel compounds by lowering the interaction strength between holo-H12 and the LBD surface. However, the difference in the directionality of the alkoxy side chains and the more constrained environment of the C4′ substitution most likely explain the lower binding affinities and the weaker agonistic activities of compounds

Table 1. Data Collection and Refinement Statistics

	RXRα/CD3254/TIF-2
Data Collection	
space group	P43212
cell dimensions	
a, *b*, *c* (Å)	65.76, 65.76, 110.86
resolution (Å)	31.53−2.00 (2.11−2.00)[a]
R_{sym}	0.077 (0.377)
$I/I\sigma$	8.6 (2.0)
completeness (%)	99.9 (100.0)
redundancy	6.0 (6.2)
Refinement	
resolution (Å)	31.53−2.00
no. reflections	16134
R_{work}/R_{free}	0.205/0.241
no. atoms	
protein	1752
ligand	27
water	112
B factors	
protein	18.94
ligand	14.84
water	24.82
rms deviations	
bond lengths (Å)	0.010
bond angles (deg)	1.166

[a] Highest resolution shell.

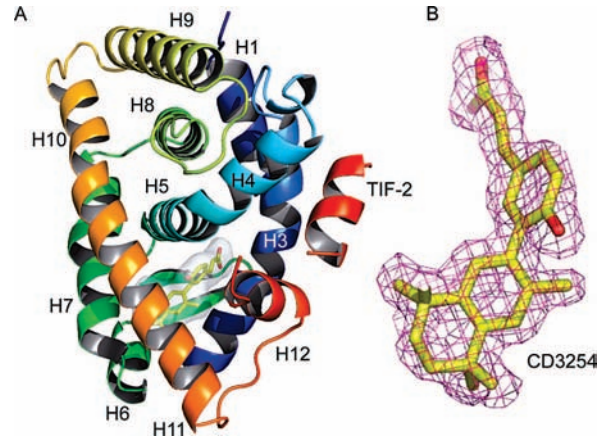

Figure 4. X-ray structure of RXRα LBD bound by **9**. (A) Overall structure of RXRα LBD in complex with **9**. Helices are numbered from N- to C-terminus. Together, helices H3, H4, and H12 define the activation function 2 (AF-2) surface to which the TIF-2 peptide is bound. (B) Experimental $2F_o - F_c$ electron density of ligand **9** contoured at 1σ.

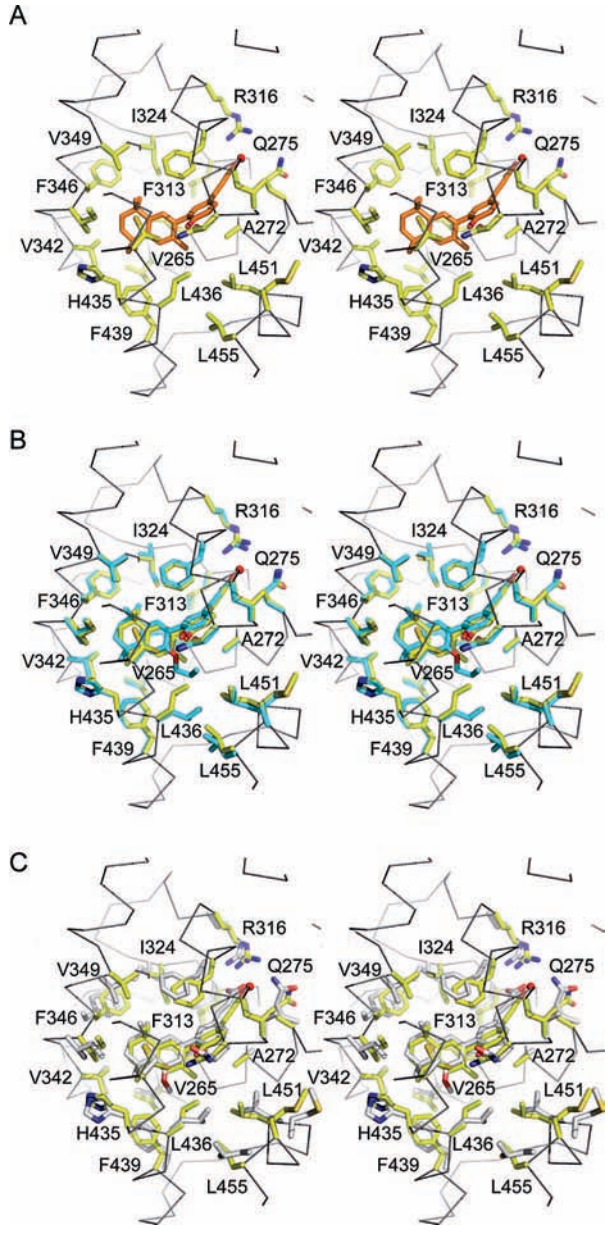

Figure 5. Structural basis of partial agonist action. (A) Close-up stereo view showing the ligand-binding pocket of RXRα bound to **9**. For clarity, C269 and I447 are not displayed. (B) Superposition of the RXRα ligand-binding pocket bound by **9** (yellow) and **10c** (blue, PDB code 2p1v). (C) Superposition of the RXRα ligand-binding pocket bound by **9** (yellow) and a docking model of **11a** bound to RXRα.

11a−**f** as compared to those of the equivalent compounds in the C3′ series **10a**−**f** (Figure 3A,B).

Conclusion

Chemical modifications at the C3′ or C4′ positions of **9** have provided two series of analogues for which the receptor activation profiles have been determined. C3′ derivatives[26] display a wide panel of activities ranging from partial agonists with a significant residual agonist activity (**10a**) to full antagonists (**10e**,**f**). Repositioning the alkyl ether chain to the C4′ position provided a much more restricted range of functional profiles and led to a decrease in both the binding affinity and the overall activity of compounds (**11a**−**f**). Indeed, all members of this isomeric series behave as weak or very weak partial agonists as judged from anisotropy and transient transactivation experiments. The present study confirms the importance of the conformation of L436 (H11) observed in the RXRα LBD/**9** structure for full agonism. Perturbation of this conformation by compounds **10a**−**f** and **11a**−**f** resulted in a decline of agonistic activity. However, it appears that L436 repositioning alone is not sufficient to confer full antagonist activity as compounds of the **11a**−**f** series retain some degree of agonist activity. Thus, full antagonism is only observed for compounds **10e**,**f**, whose long hydrophobic extensions induce a steric blockade of holo-H12 packing.[26] Moving the alkoxy side chain from C3′ to C4′ increases the distance to H12 and most likely prevents compounds **11e**,**f** from interfering directly with this helix.

This study provides important additional SAR information which contributes to the exploration of the chemical space of this type of rexinoids and reveals the subtle chemical and structural properties required to confer full or partial RXR agonistic or antagonistic activities. Accumulation of such structure-based knowledge will facilitate the design of RXR modulators optimized for the prevention and treatment of cancer or metabolic diseases.

Experimental Section

For general procedures, see Supporting Information. All compounds were purified by flash chromatography and ≥95% purity was established by combustion analysis.

Ethyl 3-(4-Acetoxy-3-bromophenyl)acrylate (16). A solution of ethyl 2-phosphonoacetate (1.31 g, 7.24 mmol) in DME (13 mL) was added to NaH (0.29 g, 7.24 mmol) at −30 °C, and the mixture was stirred for 30 min. A solution of 4-acetoxy-3-bromobenzaldehyde **15** (1.60 g, 6.58 mmol) was slowly added, and stirring was continued for 1.5 h at the same temperature. The mixture was poured onto H_2O and extracted with ether (3×). The organic extracts were washed with an aqueous saturated NH_4Cl solution (3×) and with brine, dried over Na_2SO_4, filtered, and concentrated to dryness. The residue was purified by chromatography (silicagel, 90:10 hexane/EtOAc) to afford 1.96 g (95% yield) of ester **16** as a white solid (mp 71−72 °C, hexane/EtOAc). ^{1}H NMR ($CDCl_3$, 400.13 MHz) δ 1.33 (t, J = 7.0 Hz, 3H, $CH_2\underline{CH_3}$), 2.36 (s, 3H, CH_3), 4.25 (q, J = 7.0 Hz, 2H, $C\underline{H_2}CH_3$), 6.39 (d, J = 16.0 Hz, 1H, H_2), 7.15 (d, J = 8.4 Hz, 1H, $H_{5'}$), 7.46 (dd, J = 8.4, 2.0 Hz, 1H, $H_{6'}$), 7.58 (d, J = 16.0 Hz, 1H, H_3), 7.76 (d, J = 2.0 Hz, 1H, $H_{2'}$). ^{13}C NMR ($CDCl_3$, 100.62 MHz) δ 14.3 (q), 20.8 (q), 60.7 (t), 116.9 (s), 119.9 (d), 124.1 (d), 128.0 (d), 132.6 (d), 134.0 (s), 141.9 (d), 149.4 (s), 166.4 (s), 168.3 (s). IR (NaCl): υ 2975 (m, C−H), 1772 (s, C═O), 1710 (s, C═O), 1640 (m), 1488 (m), 1177 (s) cm^{-1}. MS (EI$^+$): m/z (%) 314 ([M]$^+$, 5), 312 ([M]$^+$, 5), 272 (98), 270 (100), 244 (20), 242 (22), 227 (94), 225 (97), 200 (61), 198 (77), 147 (21), 146 (94), 145 (25), 118 (94), 117 (18), 90 (13), 89 (92). HRMS: calcd for $C_{13}H_{13}{}^{79}BrO_4$ [M]$^+$: 311.9997; found: 311.9984.

Ethyl 3-[4-Hydroxy-3-(3,5,5,8,8-pentamethyl-5,6,7,8-tetrahydronaphthalen-2-yl)-phenyl]acrylate (18). In a Schlenk flask, $Pd(OAc)_2$ (2 mg, 0.006 mmol) was added to a degassed solution of bromide **16** (50 mg, 0.159 mmol), boronic acid **12** (40 mg, 0.159 mmol), TBAB (52 mg, 0.159 mmol), and Na_2CO_3 (51 mg, 0.479 mmol) in H_2O (0.32 mL), and the resulting solution was stirred for 15 min. The reaction mixture was heated to 150 °C for 5 min to afford a dark solution. After cooling down to 25 °C, water was added and the solution was extracted with EtOAc (3×). The combined organic extracts were washed with an aqueous saturated $NaHCO_3$ solution, dried over Na_2SO_4, and evaporated to dryness. The residue was purified by chromatography (silicagel, 85:15 hexane/EtOAc) to afford 31 mg of **18**, 15 mg of acetate **17**, and 15 mg of unreacted starting material (97% yield based on recovered starting material). Data for **18**: ^{1}H NMR ($CDCl_3$, 400.13 MHz) δ 1.32 (s, 6H, 2 × CH_3), 1.33 (t, J = 7.4 Hz, 3H, $CH_2\underline{CH_3}$), 1.33 (s, 6H, 2 × CH_3), 1.71 (s, 4H, 2 × CH_2), 2.11 (s, 3H, CH_3), 4.23 (q, J = 7.4 Hz, 2H, $C\underline{H_2}CH_3$), 5.12 (br s, 1H, OH), 6.28 (d, J = 16.0 Hz, 1H, H_2), 7.00 (d, J = 8.5 Hz, 1H), 7.14 (s, 1H), 7.24 (s, 1H), 7.33 (d, J = 2.2 Hz, 1H), 7.47 (dd, J = 8.5, 2.2 Hz, 1H), 7.67 (d,

J = 16.0 Hz, H_3). ^{13}C NMR ($CDCl_3$, 100.62 MHz) δ 14.3 (q), 19.4 (q), 31.8 (q, 2×), 31.9 (q, 2×), 34.0 (s), 34.1 (s), 35.0 (t, 2×), 60.3 (t), 115.7 (d), 115.8 (d), 127.0 (s), 128.4 (d), 128.6 (s), 128.9 (d), 129.0 (d), 130.5 (d), 131.7 (s), 133.8 (s), 143.5 (s), 144.3 (d), 145.7 (s), 154.8 (s), 167.3 (s). IR (NaCl): υ 3500−3100 (br, O−H), 2960 (s, C−H), 2924 (s, C−H), 2859 (w), 1690 (s, C═O), 1631 (m), 1499 (m), 1271 (s), 1168 (s) cm^{-1}. MS (EI$^+$): *m*/*z* (%) 392 ([M]$^+$, 48), 378 (27), 377 (100). HRMS: calcd for $C_{26}H_{32}O_3$ [M]$^+$: 392.2351; found: 392.2365.

3-[4-Hydroxy-3-(3,5,5,8,8-pentamethyl-5,6,7,8-tetrahydronaphthalen-2-yl)-phenyl]acrylic Acid (9). A solution of LiOH·H_2O (82 mg, 2.0 mmol) in dioxane (2 mL) was added to ester **18** (77 mg, 0.2 mmol), and the mixture was heated to 60 °C for 3.5 h. After cooling down to 25 °C, 10% HCl was added and the mixture was extracted with EtOAc (3×). The combined organic layers were washed with H_2O and brine, dried over Na_2SO_4, filtered, and evaporated to dryness. The residue was purified by chromatography (silicagel, 60:40 hexane/EtOAc) to afford acid **9** (60 mg, 85% yield) as a white solid (mp 275 °C, hexane/EtOAc). ^{1}H NMR ($CDCl_3$, 400.13 MHz) δ 1.16 (s, 6H, 2 × CH_3), 1.23 (s, 6H, 2 × CH_3), 1.61 (s, 4H, 2 × CH_2), 2.01 (s, 3H, CH_3), 6.21 (d, J = 15.9 Hz, 1H), 6.92 (d, J = 8.4 Hz, 1H), 7.04 (s, 1H), 7.15 (s, 1H), 7.25 (d, J = 2.2 Hz, 1H), 7.38 (dd, J = 8.4, 2.2 Hz, 1H), 7.66 (d, J = 15.9 Hz, 1H). ^{13}C NMR ($CDCl_3$, 100.62 MHz) δ 19.4 (q), 31.8 (q, 2×), 31.9 (q, 2×), 34.0 (s), 34.1 (s), 35.0 (t, 2×), 114.7 (d), 115.9 (d), 126.7 (s), 128.4 (d), 128.7 (s), 128.9 (d), 129.5 (d), 130.8 (d), 131.6 (s), 133.9 (s), 143.6 (s), 145.8 (s), 146.8 (d), 155.3 (s), 172.6 (s). IR (NaCl): υ 3500−3100 (br, −OH), 2960 (s, C−H), 2926 (s, C−H), 2862 (m, C−H), 1684 (s, C═O), 1627 (m), 1601 (m), 1495 (m), 1424 (m), 1271 (s), 1174 (m), 1128 (w), 758 (m) cm^{-1}. MS (FAB$^+$): *m*/*z* (%) 364 ([M]$^+$, 47), 350 (25), 349 (100). HRMS: calcd for $C_{24}H_{28}O_3$ [M]$^+$: 364.2038; found: 364.2037.

7-Bromo-5-methoxy-1,1,4,4-tetramethyl-1,2,3,4-tetrahydronaphthalene (20a). General Procedure for the Williamson Ether Synthesis. A solution of naphthol **19** (0.40 g, 1.41 mmol) in DMF (1.8 mL) was added to NaH (85 mg, 60% in mineral oil, 2.12 mmol) at 0 °C. After stirring for 30 min, a solution of iodomethane (0.13 mL, 2.12 mmol) in DMF (0.5 mL) was added. The reaction mixture was allowed to warm up to 25 °C, and stirring was maintained for 2 h. The reaction mixture was poured over water and extracted with ether (3×). The organic extracts were washed with brine, dried over Na_2SO_4, filtered, and evaporated to dryness. The residue was purified by flash chromatography (silica gel, 98:2 hexane/EtOAc) to afford **20a** (0.39 g, 92% yield) as a white powder, mp 92−94 °C (hexane/EtOAc). ^{1}H NMR ($CDCl_3$, 400.13 MHz) δ 1.26 (s, 6H, 2 × CH_3), 1.34 (s, 6H, 2 × CH_3), 1.62 (m, 4H, 2 × CH_2), 3.79 (s, 3H, −O-CH_3), 6.79 (s, 1H), 7.07 (s, 1H). ^{13}C NMR ($CDCl_3$, 100.62 MHz) δ 28.2 (q, 2×), 31.8 (q, 2×), 34.1 (s), 34.7 (t), 34.9 (s), 37.8 (t), 55.2 (t), 112.2 (d), 119.6 (s), 122.4 (d), 132.1 (s), 149.1 (s), 159.4 (s). IR (NaCl): ν 2956 (s, C−H), 2928 (s, C−H), 2862 (m, C−H), 2361 (m), 1569 (s), 1453 (s), 1362 (s), 1268 (m), 1203 (s), 1056 (s) cm^{-1}. MS (EI$^+$): *m*/*z* (%) 298 ([M]$^+$, 24), 296 ([M]$^+$, 25), 284 (15), 283 (99), 282 (15), 281 (100), 202 (23), 187 (15), 173 (15), 160 (26). HRMS: calcd for $C_{15}H_{21}{}^{79}BrO$ [M]$^+$: 296.0776; found: 296.0768. Elemental anal. calcd (%) C 60.61, H 7.12, Br 26.88, O 5.38; found: C 60.64, H 7.31.

4-Methoxy-5,5,8,8-tetramethyl-5,6,7,8-tetrahydronaphthalen-2-ylboronic Acid (21a). General Procedure for Boronic Acid Formation. *n*-BuLi (1.19 mL, 1.22 M in hexane, 1.46 mmol) was slowly added to a solution of bromide **20a** (0.39 g, 1.32 mmol) and TMEDA (0.44 mL, 5.29 mmol) in THF (4 mL) at −78 °C. After stirring the mixture for 10 min at −78 °C, a solution of B(O^{i}Pr)$_3$ (0.92 mL, 3.97 mmol) in THF (0.5 mL) was slowly added via cannula, and stirring was maintained for 2 h at the same temperature. Then 10% HCl (5 mL) was added, and the resulting mixture was stirred for 2 h before addition of CH_2Cl_2. The aqueous layer was extracted with CH_2Cl_2 (3×), and the combined organic extracts were washed with brine, dried over Na_2SO_4, filtered, and evaporated to dryness. The residue was purified by flash chromatography (silica gel, 70:30 hexane/EtOAc) to afford **21a** (0.24 g, 69% yield) as a white powder. It was fully characterized as its diethylamino adduct as indicated below.

2-(4-Methoxy-5,5,8,8-tetramethyl-5,6,7,8-tetrahydronaphthalen-2-yl)-1,3,6,2-dioxazaborocane (22a). General Procedure for Formation of the Diethanolamine Boronates. A solution of diethanolamine in THF (0.32 mL, 0.45 M, 0.14 mmol) was added dropwise to boronic acid **21a** (30 mg, 0.11 mmol) at 25 °C. After stirring for 1 h, a white precipitate formed, which was filtered off, washed with hexane, and kept under vacuum for 2 h, to afford **22a** (38 mg, 100% yield) as a white powder, mp 253−254 °C (hexane/EtOAc). ^{1}H NMR ($CDCl_3$, 400.13 MHz) δ 1.26 (s, 6H, 2 × CH_3), 1.33 (s, 6H, 2 × CH_3), 1.60 (m, 4H, 2 × CH_2), 2.5−2.6 (br s, 2H, CH_2), 3.0−3.2 (br s, 2H, CH_2), 3,7−3.9 (br s, 3H, −O-CH_3, 4H, 2 × CH_2), 5.2−5.3 (br s, 1H, NH), 6.86 (s, 1H), 7.13 (s, 1H). ^{13}C NMR ($CDCl_3$, 100.62 MHz) δ 28.7 (q, 2×), 32.2 (q, 2×), 34.1 (s), 34.5 (s), 35.4 (t), 38.1 (t), 51.2 (t), 55.1 (q), 63.2 (t), 112.9 (d), 123.4 (d, 2×), 132.1 (s), 145.9 (s), 158.2 (s). IR (NaCl): ν 3200−3000 (br, N−H), 2951 (s, C−H), 2924 (s, C−H), 2858 (s, C−H), 2361 (m), 1458 (m), 1388 (m), 1273 (s), 1217 (s), 1102 (s), 1066 (s) cm^{-1}. MS (EI$^+$): *m*/*z* (%) 331 ([M]$^+$, 34), 316 (43), 315 (12), 300 (28), 218 (21), 204 (16), 203 (100), 161 (15), 114 (63), 113 (16), 69 (20). HRMS: calcd for $C_{19}H_{30}BNO_3$ [M]$^+$: 331.2319; found: 331.2311.

(*E*)-Ethyl 3-[4-Hydroxy-3-(4-methoxy-5,5,8,8-tetramethyl-5,6,7,8-tetrahydronaphthalen-2-yl)phenyl]acrylate (23a). General Procedure for Suzuki Cross-Coupling. In a Schlenk flask, Pd(PPh$_3$)$_4$ (19 mg, 0.016 mmol) was added to a degassed solution of bromide **16** (0.17 mg, 0.54 mmol), boronic acid **21a** (0.21 g, 0.81 mmol), and Na_2CO_3 (0.99 mL, 3 M in H_2O, 2.97 mmol) in DME (9 mL), and the resulting mixture was stirred for 15 min at 25 °C and then heated to reflux for 23 h. After cooling down to 25 °C, a 10% aqueous HCl solution was added until pH 1, and the aqueous layer was extracted with EtOAc (3×). The combined organic layers were washed with an aqueous saturated $NaHCO_3$ solution, dried over Na_2SO_4, and evaporated. The residue was purified by flash chromatography (silica gel, 85:15 hexane/EtOAc) to afford **23a** (0.12 g, 57% yield) as a white foam. ^{1}H NMR ($CDCl_3$, 400.13 MHz) δ 1.31 (s, 6H, CH_3), 1.34 (t, J = 7.0 Hz, 3H, CH_3), 1.43 (s, 6H, 2 × CH_3), 1.6−1.7 (m, 4H, 2 × CH_2), 3.84 (s, 3H, OCH_3), 4.26 (q, J = 7.2 Hz, 2H), 5.87 (br s, 1H, OH), 6.34 (d, J = 15.9 Hz, 1H, H_2), 6.73 (d, J = 1.7 Hz, 1H), 7.01 (d, J = 9.2 Hz, 1H), 7.03 (d, J = 1.7 Hz, 1H), 7.4−7.5 (m, 2H), 7.68 (d, J = 15.9 Hz, 1H, H_2). ^{13}C NMR ($CDCl_3$, 100.62 MHz) δ 14.3 (q), 28.3 (q, 2×), 31.9 (q, 2×), 34.3 (s), 34.7 (s), 34.9 (t), 37.8 (t), 55.2 (q), 60.3 (t), 109.1 (d), 115.8 (d), 116.2 (d), 119.6 (d), 122.1 (s), 127.2 (s), 128.9 (d), 129.1 (s), 130.0 (d), 133.4 (s), 133.7 (s), 144.3 (d), 148.7 (s), 154.6 (s), 159.6 (s), 167.4 (s). IR (NaCl): ν 3500−3100 (br, O−H), 2957 (s, C−H), 2929 (s, C−H), 2862 (m, C−H), 1684 (s), 1632 (s), 1599 (s), 1396 (m), 1283 (s), 1180 (s), 1048 (m) cm^{-1}. MS (EI$^+$): *m*/*z* (%) 409 ([M + H]$^+$, 28), 408 ([M]$^+$, 100), 395 (11), 394 (66), 393 (89), 393 (75), 363 (11). HRMS: calcd for $C_{28}H_{36}O_4$ [M]$^+$: 408.2304; found: 408.2301.

(*E*)-3-[4-Hydroxy-3-(4-methoxy-5,5,8,8-tetramethyl-5,6,7,8-tetrahydronaphthalen-2-yl)phenyl]acrylic Acid (11a). General Procedure for Ester Hydrolysis. A 2 M solution of KOH in MeOH (8 mL) was added to ester **23a** (100 mg, 0.24 mmol), and the mixture was heated to reflux for 2 h. After cooling down to 25 °C, a 10% aqueous HCl solution was added and the mixture was extracted with CH_2Cl_2 (3×). The combined organic layers were washed with H_2O and brine, dried over Na_2SO_4, filtered, and evaporated to dryness. The residue was purified by flash chromatography (silica gel, 90:10 CH_2Cl_2/MeOH) to afford **11a** (93 mg, 99% yield) as a white powder, mp 215−217 °C (CH_2Cl_2/hexane). ^{1}H NMR ($CDCl_3$, 400.13 MHz) δ 1.29 (s, 6H, 2 × CH_3), 1.41 (s, 6H, 2 × CH_3), 1.6−1.7 (m, 4H, 2 × CH_2), 3.83 (s, 3H, OCH_3), 6.34 (d, J = 16.0 Hz, 1H, H_2), 6.69 (s, 1H), 6.9−7.1 (m, 2H), 7.4−7.5 (m, 2H), 7.75 (d, J = 16.0 Hz, 1H, H_3). ^{13}C NMR ($CDCl_3$, 100.62 MHz) δ 28.3 (q, 2×), 32.0 (q, 2×), 34.3 (s), 34.8 (s), 34.9 (t), 37.9 (t), 55.2 (t), 109.0 (d), 115.2 (d), 116.3 (d), 119.5 (d), 127.0 (s), 129.0 (s), 129.3 (d), 130.3 (d), 133.5 (s), 133.6 (s), 146.5 (d), 148.9 (s), 154.9 (s), 159.7 (s), 172.7 (s). IR (NaCl): ν 3500−2600 (br, O−H), 2956 (s,

C−H), 2927 (s, C−H), 2860 (m), 1683 (s, C═O), 1628 (m), 1601 (m), 1501 (s), 1428 (m), 1360 (m), 1283 (s), 1184 (s) cm^{-1}. MS (EI^+): *m*/*z* (%) 380 ($[M]^+$, 33), 366 (25), 365 (100). HRMS: calcd. for $C_{24}H_{28}O_4$ $[M]^+$: 380.1988; found: 380.1982. Elem. anal. calcd for $C_{26}H_{32}O_4 \cdot H_2O$ (%) C 72.34, H 7.59; found: C 72.18, H 7.17.

Steady-State Fluorescence Anisotropy. The RARα-RXRα LBD fluorescent heterodimer has been prepared as previously described.[26] Fluorescence anisotropy assays were performed using a Safire^2 microplate reader (TECAN) at a protein concentration of 0.120 μM. The excitation wavelength was set at 470 nm, with emission measured at 530 nm. The TIF-2 NR2 coactivator peptide (686-KHKILHRLLQDSS-698) was added to protein samples containing 10 μM of ligand to a final concentration of 10 μM and then the sample was diluted successively with buffer C supplemented with 0.120 μM of heterodimer and 10 μM of ligand. At least three independent measurements were made for each sample.

Cell Culture and Determination of RXR Activity. Gal4-hRXRβ engineered HeLa cells (stably transfected with $(Gal4)_5$-βGlo-Luc-Neo reporter and Gal4-hRXRβ plasmid) were maintained in DMEM containing 5% FCS, supplemented with Geneticin G418 (0.8 mg/mL), puromycin (0.3 μg/mL), hygromycin (0.2 mg/mL), and gentamycin (40 μg/mL). To determine the transcriptional potential of the compounds, equal aliquots of cells were seeded in a 96-well plate and were incubated at 37 °C and 5% CO_2 and exposed to the ligands for 16 h (overnight). The cells were washed (PBS) and lysed (50 μL of lysis buffer: 25 mM Tris phosphate (pH 7.8), 2 mM EDTA, 1 mM DTT, 10% glycerol, and 1% Triton X-100) for 15 min. Equal aliquots (25 μL) of the cell lysates were transferred in Optiplate-96, and the luminescence in RLU was determined on a MicroLumat LB96P luminometer (Berthold) after automatic injection of 50 μL of luciferin buffer (20 mM Tris phosphate (pH 7.8), 1.07 mM $MgCl_2$, 2.67 mM $MgSO_4$, 0.1 mM EDTA, 33.3 mM DTT, 0.53 mM ATP, 0.47 mM luciferin, and 0.27 mM CoA).

Crystal Structure of the RXRα/9/TIF-2 Complex. Protein expression and purification have been described previously.[26] Briefly, the histidine-tagged LBD of human RXRα (residues 223−462 in a pET15b vector) was purified with a Ni^{2+}-affinity column followed by a gel filtration step. Fractions containing RXRα LBD were pooled, concentrated, and mixed with a 3-fold molar excess of CD3254 and a 5-fold molar excess of the TIF-2 NR2 coactivator peptide (686-KHKILHRLLQDSS-698). Crystals were obtained by vapor diffusion at 20 °C. The well buffer contained 20% PEG 4000; 0.1 M Tris.HCl, pH 8.0; 1.0 M ammonium acetate. Crystals were of space group *P*43212. A single crystal was mounted from mother liquor onto a cryoloop (Hampton research), soaked in the reservoir solution containing an additional 20% glycerol, and quickly frozen in liquid nitrogen. Diffraction data were collected using an ADSC Quantum Q210 detector at the ID14-EH1 beamline of ESRF (France) at 2.0 Å resolution. Diffraction data were processed using MOSFLM[39] and scaled with SCALA from the CCP4 program suite.[40] The structures was solved by using the previously reported structure 1MVC[37] of which the ligand and the coactivator peptide were omitted. Initial $F_o - F_c$ difference maps had strong signals for the ligand and the TIF-2 NR2 peptide, which could be fitted accurately into the electron density. The structure was modeled with COOT[41] and refined with REFMAC5[40] using rigid body, least-squares, and individual B-factor refinements. The final model exhibit very good geometry with 95.9% of the residues in the most favored regions of the Ramachandran plot and no residue in the disallowed regions.

Acknowledgment. We thank Claudine Gaudon and Audrey Bindler for the RXR reporter cells and assistance in the analysis. This work was supported by funds from the EC (QLK-2002-02029 "Anticancer Retinoids" and LSHC-CT-2005-518417 "EPITRON" to A.R.de L. and H.G.), the Spanish MEC (SAF04-07131, FEDER to A.R.de L.; Juan de la Cierva contract to F.R.-B.; SAF07-63880), the Institut National du Cancer (H.G.), the Ligue contre le Cancer ("Equipe labellisée La Ligue") (H.G.), and the French National Research Agency (ANR-07-PCVI-0001-01 to W.B.).

Note Added after ASAP Publication. This paper was released ASAP on May 1, 2009 with an error in Figure 1. The revised version was published on May 6, 2009.

Supporting Information Available: General experimental procedures, synthesis, and characterization of intermediate compounds (**14**, **19**, **20b−f**, **21b−f**, **22b−f**, **23b−f**, **11b−f**) and molecular modeling. This material is available free of charge via the Internet at http://pubs.acs.org.

References

(1) Laudet, V.; Gronemeyer, H. *The Nuclear Receptor Facts Book*; Academic Press: San Diego, 2002.
(2) Germain, P.; Staels, B.; Dacquet, C.; Spedding, M.; Laudet, V. Overview of Nomenclature of Nuclear Receptors. *Pharmacol. Rev.* **2006**, *58*, 685–704.
(3) de Urquiza, A. M.; Liu, S.; Sjöberg, M.; Zetterström, R. H.; Griffiths, W.; Sjövall, J.; Perlmann, T. Docosahexaenoic Acid, A Ligand for the Retinoid X Receptor in Mouse Brain. *Science* **2000**, *290*, 2140–2144.
(4) Calléja, C.; Messaddeq, N.; Chapellier, B.; Yang, H.; Krezel, W.; Li, M.; Metzger, D.; Mascrez, B.; Ohta, K.; Kagechika, H.; Endo, Y.; Mark, M.; Ghyselinck, N. B.; Chambon, P. Genetic and Pharmacological Evidence that a Retinoic Acid Cannot be the RXR-activating Ligand in Mouse Epidermis Keratinocytes. *Genes Dev.* **2006**, *20*, 1525–1538.
(5) Mangelsdorf, D. A.; Evans, R. M. The RXR Heterodimers and Orphan Receptors. *Cell* **1995**, *83*, 841–850.
(6) Gronemeyer, H.; Gustafsson, J.-A.; Laudet, V. Principles for Modulation of the Nuclear Receptor Superfamily. *Nat. Rev. Drug Discovery* **2004**, *3*, 950–964.
(7) Chen, J.-Y.; Clifford, J.; Zusi, C.; Starret, J.; Tortolani, D.; Ostrowski, J.; Reczec, P. R.; Chambon, P.; Gronemeyer, H. Two Distinct Actions of Retinoid−Receptor Ligands. *Nature* **1996**, *382*, 819–822.
(8) Germain, P.; Iyer, J.; Zechel, C.; Gronemeyer, H. Co-regulator Recruitment and the Mechanism of Retinoic Acid Receptor Synergy. *Nature* **2002**, *415*, 187–192.
(9) Nagy, L.; Schwabe, J. W. R. Mechanism of the Nuclear Receptor Molecular Switch. *Trends Biomed. Sci.* **2004**, *29*, 317–324.
(10) Shulman, A. I.; Larson, C.; Mangelsdorf, D. J.; Ranganathan, R. Structural Determinants of Allosteric Ligand Activation in RXR Heterodimers. *Cell* **2004**, *116*, 417–429.
(11) Mukherjee, R.; Davies, P. J. A.; Crombie, D. L.; Bischoff, E. D.; Cesario, R. M.; Jow, L.; Hamann, L. G.; Boehm, M. F.; Mondon, C. E.; Nadzan, A. M.; Paterniti, J. R.; Heyman, R. A. Sensitization of Diabetic and Obese Mice to Insulin by Retinoid X Receptor Agonists. *Nature* **1997**, *386*, 407–410.
(12) Altucci, L.; Leibowitz, M. D.; Ogilvie, K. M.; de Lera, A. R.; Gronemeyer, H. RAR and RXR Modulation in Cancer and Metabolic Disease. *Nat. Rev. Drug Discovery* **2007**, *6*, 793–810.
(13) Liby, K. T.; Yore, M. M.; Sporn, M. B. Triterpenoids and Rexinoids as Multifunctional Agents for the Prevention and Treatment of Cancer. *Nat. Rev. Cancer* **2007**, *7*, 357–369.
(14) Dawson, M. I.; Zhang, X. -k. Discovery and Design of Retinoic Acid Receptor and Retinoid X Receptor Class- and Subtype-Selective Synthetic Analogs of All-*trans*-retinoic Acid and 9-*cis*-Retinoic Acid. *Curr. Med. Chem.* **2002**, *9*, 623–637.
(15) Kagechika, H.; Shudo, K. Synthetic Retinoids: Recent Developments Concerning Structure and Clinical Utility. *J. Med. Chem.* **2005**, *48*, 5875–5883.
(16) Hashimoto, Y.; Miyachi, H. Nuclear Receptor Antagonists Designed Based on the Helix-folding Inhibition Hypothesis. *Bioorg. Med. Chem.* **2005**, *13*, 5080–5093.
(17) Lala, D. S.; Mukherjee, R.; Shulman, I. G.; Canan Koch, S. S.; Dardashti, L. J.; Nadzan, A. M.; Croston, G. E.; Evans, R. M.; Heyman, R. A. Activation of Specific RXR Heterodimers by an Agonist of RXR Homodimers. *Nature* **1996**, *383*, 450–453.
(18) Gernert, D. L.; Ajamie, R.; Ardecky, R. A.; Bell, M. G.; Leibowitz, M. D.; Mais, D. A.; Mapes, C. M.; Michellys, P. Y.; Rungta, D.; Reifel-Miller, A.; Tyhonas, J. S.; Yumibe, N.; Grese, T. A. Design and Synthesis of Fluorinated RXR Modulators. *Bioorg. Med. Chem. Lett.* **2003**, *13*, 3191–3195.
(19) Leibowitz, M. D.; Ardecky, R. J.; Boehm, M. F.; Broderick, C. L.; Carfagna, M. A.; Crombie, D. L.; D'Arrigo, J.; Etgen, G. J.; Faul, M. M.; Grese, T. A.; Havel, H.; Hein, N. I.; Heyman, R. A.; Jolley,

D.; Klausing, K.; Liu, S.; Mais, D. E.; Mapes, C. M.; Marschke, K. B.; Michellys, P. Y.; Montrose-Rafizadeh, C.; Ogilvie, K. M.; Pascual, B.; Rungta, D.; Tyhonas, J. S.; Urcan, M. S.; Wardlow, M.; Yumibe, N.; Reifel-Miller, A. Biological Characterization of a Heterodimer-selective Retinoid X Receptor Modulator: Potential Benefits for the Treatment of Type 2 Diabetes. *Endocrinology* **2006**, *147*, 1044–1053.

(20) Vivat, V.; Zechel, C.; Wurtz, J.-M.; Bourguet, W.; Kagechika, H.; Umemiya, H.; Shudo, K.; Moras, D.; Gronemeyer, H.; Chambon, P. A Mutation Mimicking Ligand-induced Conformational Change Yields a Constitutive RXR that Senses Allosteric Effects in Heterodimers. *EMBO J.* **1997**, *16*, 5697–5709.

(21) Sakaki, J.; Konishi, K.; Kishida, M.; Gunji, H.; Kanazawa, T.; Uchiyama, H.; Fukaya, H.; Mitani, H.; Kimura, M. Synthesis and Structure−Activity Relationship of RXR Antagonists Based on the Diazepinylbenzoic Acid Structure. *Bioorg. Med. Chem. Lett.* **2007**, *17*, 4808–4811.

(22) Sakaki, J.; Kishida, M.; Konishi, K.; Gunji, H.; Toyao, A.; Matsumoto, Y.; Kanazawa, T.; Uchiyama, H.; Fukaya, H.; Mitani, H.; Arai, Y.; Kimura, M. Synthesis and Structure−Activity Relationship of Novel RXR Antagonists: Orally Active Antidiabetic and Antiobesity Agents. *Bioorg. Med. Chem. Lett.* **2007**, *17*, 4804–4807.

(23) Takahashi, B.; Ohta, K.; Kawachi, E.; Fukasawa, H.; Hashimoto, Y.; Kagechika, H. Novel Retinoid X Receptor Antagonists: Specific Inhibition of Retinoid Synergism in RXR-RAR Heterodimers. *J. Med. Chem.* **2002**, *45*, 3327–3329.

(24) Cavasotto, C. N.; Liu, G.; James, S. Y.; Hobbs, P. D.; Peterson, V. J.; Bhattacharya, A. A.; Kolluri, S. K.; Zhang, X.-k.; Leid, M.; Abagyan, R.; Liddington, R. C.; Dawson, M. I. Determinants of Retinoid X Receptor Transcriptional Antagonism. *J. Med. Chem.* **2004**, *47*, 4360–4372.

(25) Yamauchi, T.; Kamon, J.; Waki, H.; Terauchi, Y.; Kubota, N.; Hara, K.; Mori, Y.; Ide, T.; Murakami, K.; Tsuboyama-Kasaoka, N.; Ezaki, O.; Akanuma, Y.; Gavrilova, O.; Vinson, O.; Reitman, M. L.; Kagechika, H.; Shudo, K.; Yoda, M.; Nakano, Y.; Tobe, K.; Nagai, R.; Kimura, S.; Tomita, M.; Froguel, P.; Kadowaki, T. The Fat-derived Hormone Adiponectin Reverses Insulin Resistance Associated with Both Lipoatrophy and Obesity. *Nat. Med.* **2001**, *7*, 941–946.

(26) Nahoum, V.; Pérez, E.; Germain, P.; Rodríguez-Barrios, F.; Manzo, F.; Kammerer, S.; Lemaire, G.; Hirsch, O.; Royer, C. A.; Gronemeyer, H.; de Lera, A. R.; Bourguet, W. Modulators of the Structural Dynamics of RXR to Reveal Receptor Function. *Proc. Natl. Acad. Sci. U.S.A.* **2007**, *104*, 17323–17328.

(27) Bernardon, J.-M. Preparation of Bicyclic Aromatic Compounds and their Use in Cosmetic or Dermatological Compositions. Patent EP 947496 A1 19991006, 1999.

(28) Bourguet, W.; Germain, P.; Gronemeyer, H. Nuclear Receptor Ligand-Binding Domains: Three-Dimensional Structures, Molecular interactions and Pharmacological Implications. *Trends Pharmacol. Sci.* **2000**, *21*, 381–388.

(29) de Lera, A. R.; Bourguet, W.; Altucci, L.; Gronemeyer, H. Design of Selective Nuclear Receptor Modulators: RAR and RXR as a Case Study. *Nat. Rev. Drug Discovery* **2007**, *6*, 811–820.

(30) Anderson, J. C.; Namli, H.; Roberts, C. A. Investigations into Ambient Temperature Biaryl Coupling Reactions. *Tetrahedron* **1997**, *53*, 15123–15134.

(31) Kotha, S.; Lahiri, K.; Kashinath, D. Recent Applications of the Suzuki−Miyaura Cross-coupling Reaction in Organic Synthesis. *Tetrahedron* **2002**, *58*, 9633–9695.

(32) Faul, M. M.; Ratz, A. M.; Sullivan, K. A.; Trankle, W. G.; Winneroski, L. L. Synthesis of Novel Retinoid X Receptor-Selective Retinoids. *J. Org. Chem.* **2001**, *66*, 5772–5782.

(33) Leadbeater, N. E.; Marco, M. Rapid and Amenable Suzuki Coupling Reaction in Water Using Microwave and Conventional Heating. *J. Org. Chem.* **2003**, *68*, 888–892.

(34) Tan, Y.-L.; White, A. J. P.; Widdowson, D. A.; Wilhelm, R.; Williams, D. J. Dilithiation of Arenetricarbonylchromium(0) Complexes with Enantioselective Quench: Application to Chiral Biaryl Synthesis. *J. Chem. Soc., Perkin Trans. 1* **2001**, 3269–3280.

(35) Tripathy, P. B.; Matteson, D. S. Asymmetric Synthesis of the Four Stereoisomers of 4-Methyl-3-heptanol via Boronic Esters: Sequential Double Stereodifferentiation Leads to very High Purity. *Synthesis* **1990**, 200–206.

(36) Egea, P. F.; Mitschler, A.; Rochel, N.; Ruff, M.; Chambon, P.; Moras, D. Crystal Structure of the Human RXRα Ligand-binding Domain Bound to its Natural Ligand: 9-*Cis*-retinoic Acid. *EMBO J.* **2000**, *19*, 2592–2601.

(37) Egea, P. F.; Mitschler, A.; Moras, D. Molecular Recognition of Agonist Ligands by RXRs. *Mol. Endocrinol.* **2002**, *16*, 987–997.

(38) Pogenberg, V.; Guichou, J.-F.; Vivat-Hannah, V.; Kammerer, S.; Pérez, E.; Germain, P.; de Lera, A. R.; Gronemeyer, H.; Royer, C. A.; Bourguet, W. Characterization of the Interaction Between RAR/RXR Heterodimers and Transcriptional Coactivators Through Structural and Fluorescence Anisotropy Studies. *J. Biol. Chem.* **2005**, *280*, 1625–1633.

(39) Leslie, A. G. The Integration of Macromolecular Diffraction Data. *Acta Crystallogr., Sect. D: Biol. Crystallogr.* **2006**, *62*, 48–57.

(40) The CCP4 Suite: Programs for Protein Crystallography. *Acta Crystallogr., Sect. D: Biol. Crystallogr.* **1994**, *50*, 760.

(41) Emsley, P.; Cowtan, K. Coot: Model-building Tools for Molecular Graphics. *Acta Crystallogr., Sect. D: Biol. Crystallogr.* **2004**, *60*, 2126–2132.

JM900096Q